J Mater Sci (2009) 44:6427–6436
DOI 10.1007/s10853-009-3892-y

Morphology development in nanoclay filled rubber compounds and rubber blends detected by online measured electrical conductance

Z. Ali · H. H. Le · S. Ilisch · H.-J. Radusch

Received: 25 May 2009 / Accepted: 14 September 2009 / Published online: 23 September 2009

Abstract The online measured electrical conductance (OMEC) during the rubber mixing process has been used as a novel method to characterize the dispersion of organoclay in rubber compounds and blends. This method was also used for the investigation of morphology development and kinetics of organoclay distribution in carboxylated hydrogenated nitrile butadiene rubber (XHNBR) and hydrogenated nitrile butadiene rubber (HNBR) as well as blends of HNBR with natural rubber (NR). The synchronized increase of the OMEC measured directly in the mixing chamber of the internal mixer along with dispersion of organoclay in the rubber matrix has been observed. The conductivity signal is sensitive to the intercalation/exfoliation process of organoclay in rubber compounds. The correlation between the OMEC and intercalation/exfoliation of organoclay has been determined by various offline experimental techniques like atomic force microscopy (AFM), transmission electron microscopy (TEM), and small angle X-ray scattering (SAXS). In heterogeneous blends the organoclay not only has the tendency to localize in one specific phase, but also strongly influence the development of the blend morphology, which has been nicely correlated with the OMEC chart of HNBR/(NR–clay) blends. A deeper insight into the mixing kinetics, clay transfer as well as development of the blend morphology was achieved on the basis of OMEC chart.

Z. Ali · H. H. Le (✉) · S. Ilisch · H.-J. Radusch
Center of Engineering Sciences, Polymer Technology, Martin Luther University Halle-Wittenberg, Kurt-Mothes-Str. 1, 06099 Halle, Germany
e-mail: hai.le.hong@iw.uni-halle.de

Introduction

In the last decade polymer–clay nanocomposites have attracted a substantial attention of scientists and industrialists for easy processing and cost-effective materials with improved properties. The development of nanocomposite materials opens a novel way for the preparation of new materials with pre-determined characteristics. The pristine clay consists of anionic charged layers of aluminum/magnesium silicates and small cations such as sodium or potassium located in silicate interlayer galleries [1, 2]. These cations can be exchanged with organic cationic molecules. The modification of the clay by organic ammonium ions expands the layer spacing and makes it compatible to the polymer matrix. Intercalated structures are formed when segments of the macromolecules infiltrate the expanded layers. Exfoliated structures are obtained when the clay layers are well separated and individually dispersed in the polymer matrix. The exfoliation of nano-size silicate platelets drastically increases the inner surface area of the filler and the improved interactions between clay and polymer matrix to enhanced performance of the nanocomposite especially by improved mechanical properties [3, 4], e.g., increased storage and loss moduli [5] or improved stiffness [6], reduced gas permeability [7, 8], and enhanced thermal stability [9]. Organoclay not only influences the properties of the single phase polymer matrix, but affects significantly polymer blends due to its odd distribution in the blend phases and the tendency to improve the compatibility of immiscible binary blends [10, 11]. Regarding the inhomogeneous distribution of clay in polymer blends, different works showed that clay preferentially resides in the blend phase having the better chemical affinity to clay [12–14]. If clay shows the similar affinity to both of the blend phases it concentrates dominantly at the interphase [15–17]. Some

studies of polymer blend–clay systems have also reported the compatibilizing effect of clay in immiscible blends [14, 18, 19]. Polymer–clay nanocomposites research has been mainly focused on the improving the microstructure and the impact on the material properties. Most efforts have been centered on the finding the exfoliated structure of clay either by tailoring the material and technological parameters [20–26].

The polymer–clay nanocomposites are usually characterized by offline and post-processing techniques, like transmission electron microscopy (TEM), atomic force microscopy (AFM) [21], small angle X-ray scattering (SAXS), nuclear magnetic resonance (NMR) [27], and Fourier transformed infrared spectroscopy (FT-IR) [28]. The offline experimental techniques are not only time consuming, labor intensive, expensive, requiring a high expertise, but also crucial in determining the influence of processing parameters on the resulting microstructure. Replacing the offline measurements or minimizing them with online measurement method, which would quite cost effective and easy in handling is highly desirable. The online method, reported in this article is based on electrical conductivity and has been successfully used for the qualitative and quantitative characterization of the kinetics of carbon black (CB) and carbon nanotubes (CNT) distribution in rubber compounds as well as in rubber blends [29, 30]. Some authors have reported the appearance of a conductance signal in polymer–clay nanocomposites [31–33]. The conductivity in polymer–clay nanocomposites is ionic in nature. It has been suggested that the electrical conductivity in the nanocomposites is due to the high ion transfer through inter- and intra-regions of the silicate galleries [31, 32]. It is presumed that mixing organoclay imparts the ammonium cation due to intercalation and exfoliation in the rubber matrix. Thus, the received electrical signal can be used for the investigation of the change of the clay dispersion in the host polymer during the mixing process, as shown in our preliminary work [34, 35]. Bur et al. [36] used dielectrical measurements and detected electrical signals during melt mixing of polyamide–clay nanocomposites in twin screw extrusion. This method gives information on the morphology of the nanocomposite only at one position, i.e., the position of the sensor, but it fails to display the complete spectrum of clay dispersion in the polymer matrix.

This work is focused on the development of a novel online method based on the online measured electrical conductance (OMEC) for the characterization of organoclay intercalation/exfoliation in the rubber matrix during melt mixing in an internal mixer. In fact the method delivers an efficient feedback which provides an effective way to study the kinetics of intercalation/exfoliation of organoclay, which influence the quality of the product. The data obtained has been correlated to the very well known techniques AFM, TEM, and SAXS for characterization of organoclay intercalation/exfoliation in polymer materials. The method has also been successfully applied to investigate the effect of organoclay in incompatible polar/non-polar (HNBR/NR–clay) rubber blends. It not only successfully explains the fillers phase specific localization, but also the development of blend morphology for a heterogeneous polymer blends system.

Experimental

Materials

Carboxylated hydrogenated nitrile butadiene rubber (XHNBR) Therban KA 8889 (Lanxess) with acrylonitrile content of 33% and hydrogenated nitrile butadiene rubber (HNBR) Zetpol 2030L (Zeon) with acrylonitrile content of 33% were used as host polymers for single phase rubber–clay nanocomposites. HNBR, Zetpol 2030L, and natural rubber (NR) SMR 10 (Astlett) were used as rubber matrix for the HNBR/NR blends. Organoclay Nanofil 9 (Süd-Chemie) modified by stearyl benzyl dimethyl ammonium chloride with layer spacing of 2.0 nm, an average particle size of about 35 μm, and a weight loss on ignition of 35% was used as nanofiller. Peroxide Luperox 101 (Atofina Chemicals) was used as a cross-linking agent.

Preparation of nanocomposites

The matrix was mixed with peroxide in an internal mixer Poly Lab System Rheocord (Thermo Electron/Haake) at an initial chamber temperature of 50 °C and a rotor speed of 70 rpm. Clay was added after 7 min. A clay concentration of 5 phr was kept constant for all nanocomposites. For the characterization of the dispersion kinetics of organoclay, samples were taken out after different characteristic mixing times: 1, 3, 10, and 25 min for XHNBR and 1, 4, 10 and 20 min for HNBR–clay nanocomposites. The mixing time denotes the time after addition of organoclay. The mixtures were compression-molded and vulcanized for 1 mm thick plates and analyzed.

For preparation of blend–clay nanocomposites, in the first mixing step, NR was mixed with 10 phr organoclay in an internal mixer Poly Lab System Rheocord (Thermo Electron/Haake) at an initial chamber temperature of 50 °C, rotor speed of 70 rpm for mixing time of 10 min to produce a NR–clay masterbatch. In the second step, plain HNBR was mixed with the NR–clay master batch to get 50/50 HNBR/NR blends having a clay concentration of 5 phr. In the following they are called HNBR/(NR–clay masterbatch) blend. In order to investigate the kinetics of

organoclay dispersion and development of blend morphology, the samples were taken out at different mixing times. The mixing time denotes the time after mixing of HNBR and NR–clay masterbatch. The mixtures were compression-molded and vulcanized for 1 mm thick plates and investigated.

Instrumentation

Online electrical conductance measurements

A conductivity sensor has been installed in the chamber of the internal mixer to measure the electrical conductance signal of the mix volume between the sensor and the chamber wall as used by Le et al. [29]. The construction and position of the conductivity sensor were modified to detect the conductance signal of the investigated system with good reproducibility.

Atomic force microscopy

The surface structure of a flat microtome cut surface was analyzed using a Quesant Q-Scope (Quesant), equipped with a 40 μm × 40 μm scanner. Standard cantilevers NSC 16 with a resonance frequency and force constant of about 170 kHz and 40 N m^{-1}, respectively, were used for scanning. Samples were produced by cutting in a cryo-chamber CN 30 of a rotary microtom HM 360 (Microm) with a diamond knife at −120 °C.

Transmission electron microscopy

The bulk morphology of the films was analyzed using a transmission electron microscope JEM 2010 (Jeol). Thin sections of 100 nm thickness of the cross-section of the films were prepared at -100 °C using an ultracut microtome (Leica), equipped with a 45° diamond knife.

X-ray diffraction

Small angle X-ray scattering measurements were performed at room temperature using a rotating anode X-ray source RU-3HR (Rigaku) equipped with a nickel-filtered Cu Kα tube ($\lambda = 0.154$ nm) for detection of the state of intercalation/exfoliation. The generator voltage was 40 kV and the generator current 60 mA. The scattering vector q is defined by $q = 4\pi/\lambda \sin\theta$. The first order Bragg peak in the Lorentz corrected intensity curves were fitted by using a Gaussian function with linear background subtraction, giving the interlayer distance and the relative peak strength. All samples had a uniform dimension with a thickness of 1.0 mm, i.e., the obtained peak area corresponds to the amount of ordered structures.

Results and discussion

Intercalation and exfoliation of nanoclay in XHNBR and HNBR

Figure 1a and b depicts the development of the OMEC after addition of organoclay into the XHNBR and HNBR rubber matrixes, respectively, at a rotor speed of 70 rpm. The OMEC chart indicates that the conductance increases significantly in the start of the clay addition (Fig. 1a). However, after a short time the development of the conductance declines and passes through a characteristic point (CP), then it remains constant and no change in the conductance after 12 min (CP) in XHNBR clay mixture appears. A similar behavior has been observed for HNBR–clay mixture, where CP corresponds to 4 min of mixing time (Fig. 1b). Furthermore, after CP in both of the cases the OMEC reaches a plateau, i.e., even after prolonging mixing time, no change of the OMEC can be observed. Unmodified clay does not show any conductance on addition to the rubber matrix [34],

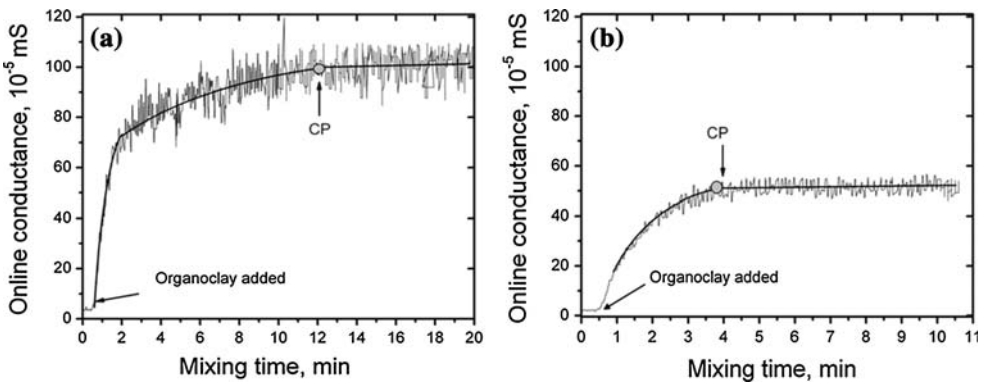

Fig. 1 Online conductance in dependence of mixing time: **a** XHNBR–clay nanocomposites, **b** HNBR–clay nanocomposites

thus the electrical conductance of the system seems to be connected to the modification of the clay for generating organophilic filler which can be easily intercalated and exfoliated, respectively.

The increase of OMEC just after addition of organocaly is related with the dispersion of the filler. The intercalation of organoclay seems to disassociate or weaken the attractive forces between the cationic end group of the alkyl ammonium molecule and the negatively charged clay surface. Sadhu et al. [37] observed that there exists hydrogen bonding between the nitrile group of the HNBR and ammonium ion of surfactants of organoclay. The steady motion of rubber chains during melt mixing of the rubber and organoclay facilitates the motion of ammonium cations and results in an increase of conductance by about two orders of magnitude in XHNBR–clay nanocomposites as compared to that of the unfilled rubber. The more the contact area between organoclay and rubber increases along the mixing time because of the ongoing intercalation and exfoliation processes, the more charge carriers released from the clay galleries into the matrix and higher electrical conductance can be observed. It is obvious that the number and size of the organoclay agglomerates decrease along the mixing time, since large clay agglomerates are broken down into smaller aggregates (tactoids). The break-up process of larger agglomerates quickly establishes new clay surface that facilitates the diffusion process of rubber chains into the clay galleries [24]. As a result, in this period wetting and intercalation of clay surface by rubber molecules mainly take place resulting in an increase of OMEC. The number of separated clay layers increases due to the progress of exfoliation process up to CP. Park and Jana [38] proposed in their study on epoxy nanocomposites that clay exfoliation starts at the surface layers of the tactoids and continues towards the center until all layers are exfoliated. Their proposed process is analogous to the erosion process as described in the "onion model" used for the explanation of the dispersion process of carbon black in a polymer matrix by Shiga and Furuta [39].

A similar behavior has been observed in case of HNBR–clay nanocomposites. Figure 1b shows that the OMEC increases after addition of organoclay, reaches the maximum value after 4 min and then remains constant. The lower level of OMEC in Fig. 1b as compared to Fig. 1a could be due to poor dispersion of organoclay in HNBR, which is less polar than XHNBR.

SAXS is most commonly used techniques for examining the clay structure and has been occasionally used for studying the kinetics of polymer nanocomposites. The intercalated and exfoliated nanostructure can be studied by monitoring the position, shape, and intensity of the basal reflection of SAXS patterns of the materials. Figure 2a and b shows that as the mixing time increases, the peak height and the area under the peak decreases. The peak height reaches the highest level after a mixing time of about 1 min due to the intercalation process. The following decrease of the peak height indicates that the regular structure of clay in the nanocomposite is destroyed, i.e., delaminated, or the clay layers are homogeneously dispersed. Consequently, it may be reasonable to mention that the organoclay is exfoliated in the polymer matrix. During melt mixing of rubber and organoclay, the intercalation and exfoliation processes take place simultaneously and they affect the height of the peak in the opposite direction, which means that increasing mixing time decreases the peak area.

Figure 2a and b shows the SAXS analysis of XHNBR–clay and HNBR–clay nanocomposites, respectively. The use of SAXS for determining the layer spacing is obvious due to periodic arrangement of the clay layers both in pristine and intercalated states. The broad peak in SAXS analysis represents the interlayer spacing of organoclay in the nanocomposites (Fig. 2a, b). The intensity of the peak, which indirectly reflects the ordered structure of the nanocomposites, changes with mixing time as shown in Fig. 2a and b. However, the position and intensity of the peak remains unchanged after the CP. The data of the clay provider as well as the investigation carried out in our labs show that the organoclay has a basal spacing of 2.0 nm

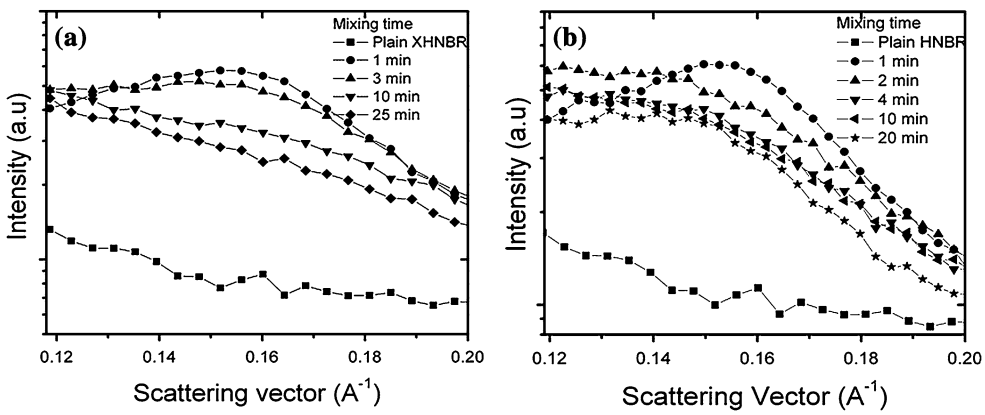

Fig. 2 SAXS analysis for samples at different mixing times: **a** XHNBR–clay nanocomposites, **b** HNBR–clay nanocomposites

before compounding. The characteristic peak at the scattering vector $q = 0.15\ A^{-1}$ corresponds to a basal spacing of about 4.2 nm of the organoclay in the nanocomposites (Fig. 2a). The peak intensity decreases with mixing time and at CP and afterwards no peak can be observed any more for XHNBR–clay nanocomposites. Whereas in case of HNBR–clay nanocomposites, the peak remains constant after 4 min of mixing time, i.e., CP, even after a long mixing time after CP the peak intensity does not change as shown in Fig. 2b. The area under the SAXS curve is high in the beginning of melt mixing. It decreases with mixing time and reaches nearly constant level at CP. Peak position ($q = 0.15\ A^{-1}$; layer spacing = 4.2 nm) and intensity remain constant after CP.

Due to such an intensive intercalation and exfoliation process, a lager amount of ionic species trapped inside the galleries could move into the rubber matrix. This is the main reason why the OMEC increases so fast in the first stage of the mixing process. Furthermore, the area under the SAXS peak becomes approximately zero at mixing time of 10 min (near CP). The disappearance of the peak in the SAXS curve behind CP means a constant morphology of totally exfoliated state which is in coincidence with OMEC that remains constant in this period. However, in case of HNBR–clay nanocomposites as shown in the Fig. 2b, the SAXS analysis shows that peak reaches to its constant value after CP. It was observed that even after the longer mixing time, the peak position and area remain constant as that for 4 min curve (CP for HNBR), which is nicely co-related with the OMEC of HNBR–clay mixtures as shown in Fig. 1b. This also supports the conjecture that lower conductance level for HNBR–clay nanocomposites is due to poor dispersion of organoclay in the HNBR matrix.

The correlation between the OMEC and organoclay dispersion on microscopic scale has been characterized by AFM. Figure 3a–c shows the morphological analysis carried out by AFM of the XHNBR–clay nanocomposites with different mixing times of 3, 10 (near CP), and 25 min, respectively. The AFM images show that at 3 min big clay agglomerates still exist in start of the mixing process. As

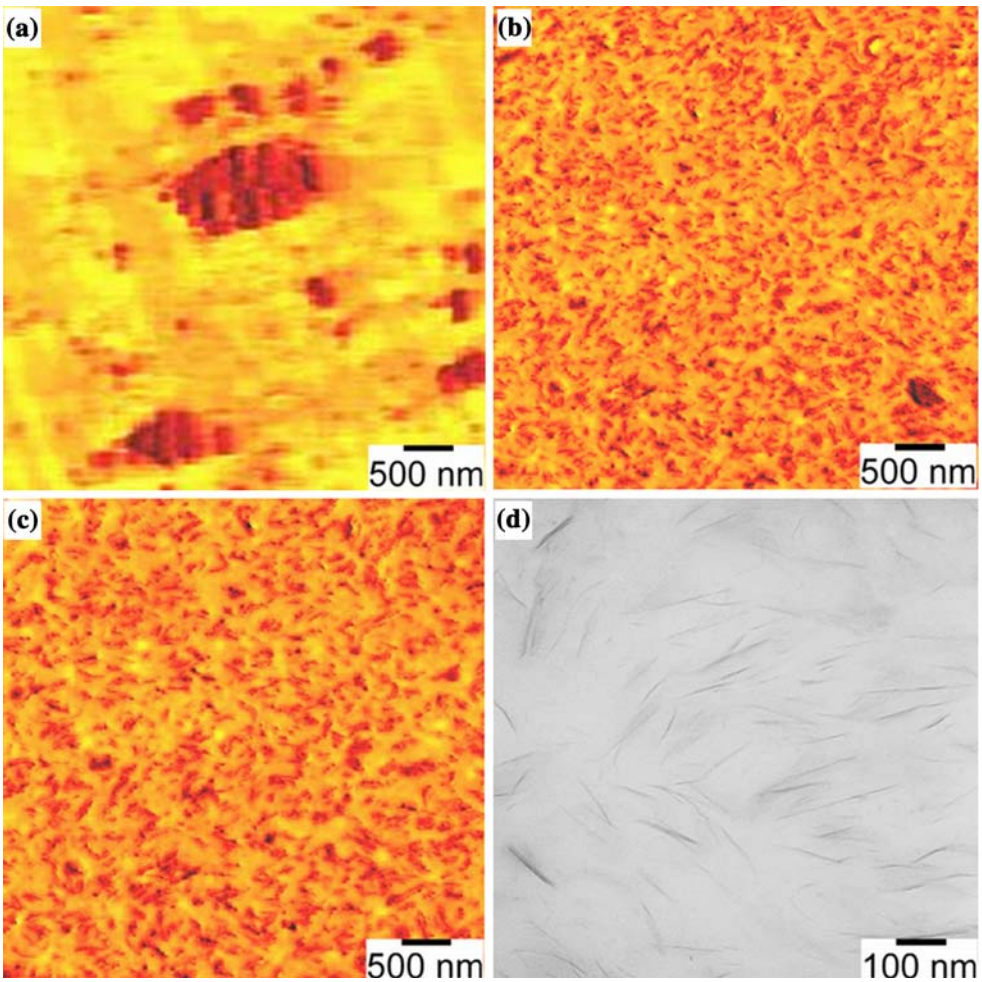

Fig. 3 AFM-images **a–c** of XHNBR–clay nanocomposites at different mixing times: **a** 3 min, **b** 10 min (near CP), **c** 25 min and TEM micrograph **d** 25 min of XHNBR–clay nanocomposites

the mixing time increases, the agglomerates are broken down into smaller tactoids and then finally exfoliated in the polymer matrix. The morphological investigation shows that a constant morphology has been reached at the characteristic point CP; even prolonging mixing time after CP does not change the morphology any more. This is correlated to Fig. 1a, i.e., OMEC also remains constant after the characteristic point.

It was observed that early morphology evolved in the beginning of the process is due to break up of agglomerates into small tactoids. The break-up process of larger agglomerates facilitates the diffusion process of rubber chains into the clay galleries [24]. As further the mixing time increases or more shear force is applied the more clay tactoids are exfoliated to clay platelets. Figure 3b and c depicts that the morphology remains constant after CP. This is in very good correlation with the OMEC, which also increases in the beginning of mixing and after CP a plateau is obtained.

Figure 3d shows the magnified TEM image at mixing time of 25 min. Clearly exfoliated platelets can be seen. It also reveals that organoclay is exfoliated in the rubber matrix. TEM results are coherent and consistent with AFM and SAXS results.

The morphology development in HNBR–clay nanocomposites with different mixing time is shown in the Fig. 4. The AFM micrographs show that the clay agglomerates are broken into smaller tactoids, which are then intercalated/exfoliated up to CP (Fig. 4a, b). It can also be analyzed that for longer mixing time, after CP, clay particles with size of about 100 nm are visible and the morphology seems to remain unchanged as shown in Fig. 4c. This shows that a constant morphology has been achieved after CP that could explain the plateau of the OMEC in this period (see Fig. 1b). Further mixing only distributes the clay aggregates more homogeneously in the polymer matrix.

Taking into account the dispersion behavior of organoclay in XHNBR and HNBR an important difference can be observed. The presence of the carboxyl groups in XHNBR strongly enhances the rubber–filler interaction and causes the appearance of the CP at about 12 min resulting in full exfoliation of organoclay in it. In HNBR there is no such strong electronegative group (carboxylic group) that leads to comparatively less interaction of filler with the elastomer, thus predominantly intercalation of clay in the elastomer is observed. Gatos et al. [40] have thoroughly investigated nanocomposites formation of HNBR as a function of surfactant types in various organoclays and found on the basis of SAXS and TEM that both intercalated/exfoliated structures are obtained. There is no complete exfoliation, however, better interaction has been observed for more polar organoclay. It has also been shown in a number of investigations that melt mixing of NBR with organoclay usually results in predominantly intercalated structures with tactoid sizes in the range of 20 nm whereas some parts of the clay were exfoliated [21, 22, 41–45]. However, complete exfoliation has not been achieved. But in this work in the case of XHNBR, predominantly exfoliation has been observed as is shown by SAXS and TEM investigations, which is due to additional strong electrophilic group, i.e. carboxylic group, in the XHNBR.

Nanofiller localization in HNBR/NR blends

The OMEC of unfilled HNBR/NR blend and HNBR/(NR–clay masterbatch) blend is shown in Fig. 5a. The OMEC curve of the unfilled 50/50 HNBR/NR blend is low because it is originated only by the HNBR component. The conductance values of pure NR or NR–clay nanocomposites are below the range of the measuring equipment and are considered as zero. Thus, when HNBR was mixed with NR–clay masterbatch it should be expected in the first range that the OMEC curve of the HNBR/(NR–clay master batch) blend will lie in the level as that of the unfilled HNBR/NR blend. However, the OMEC of the filled blend, i.e., HNBR/(NR–clay masterbatch) blend, shows a chart with very high

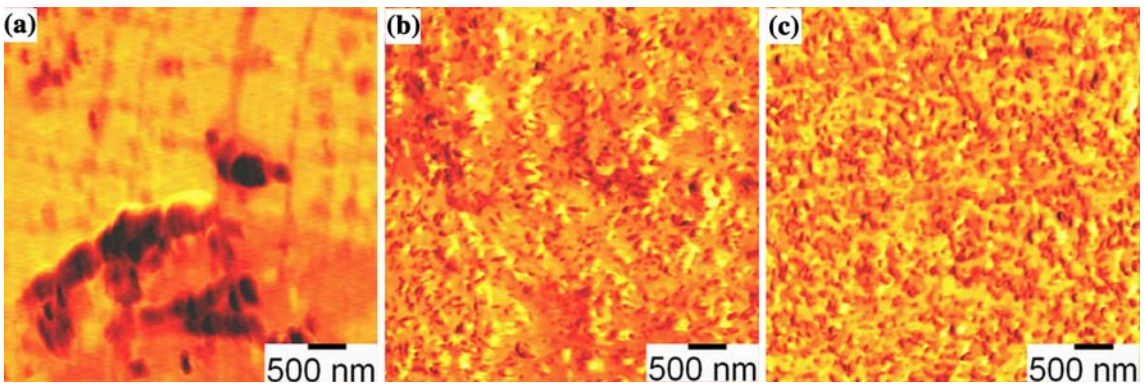

Fig. 4 AFM-images of HNBR–clay nanocomposites in dependence on mixing time: **a** 1 min, **b** 4 min (CP), **c** 20 min

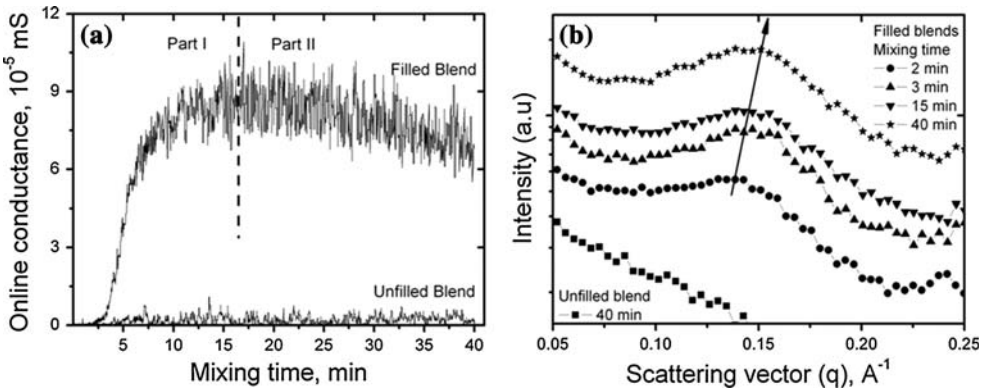

Fig. 5 **a** OMEC of the unfilled HNBR/NR blend and HNBR/(NR–clay master batch) blend nanocomposites in dependence on mixing time and **b** SAXS analysis of HNBR/(NR–clay masterbatch) blends

level compared to the unfilled HNBR/NR blend. It could be analyzed that the OMEC spectrum of filled blend is similar to that observed for XHNBR and HNBR–clay nanocomposites as shown in Fig. 1. But a decrease of OMEC curve appears after 15 min of mixing time. In order to explain the odd behavior of OMEC, the curve can be divided into two parts. First part characterizes the increase of the curve up to 15 min of mixing time. Second part describes mixing after 15 minutes to the end of melt mixing process. In order to have a deeper insight into the structural background of the OMEC curve, the organoclay dispersion and distribution in blends as well as the development of the blend morphology, the investigations have been carried out by means of AFM, TEM, and SAXS.

Figure 5b shows the normalized SAXS analysis of the unfilled HNBR/NR blend and HNBR/(NR–clay masterbatch) blends. No peak appears in the unfilled blend in the scattering vector range of 0–0.2. Organoclay-filled blends exhibit a large broad peaks correspond to the interlayer spacing of the organoclay. The shape and height of the peak do not change essentially. With longer mixing time, the whole curves shift to higher intensity values and the position of the peaks also slightly shifts to higher scattering vector values. The peak area which represents the amount of intercalated organoclay does not change. It indicates that the amount of the intercalated structure of clay in bulk remains constant even after 40 min mixing time. With increasing mixing time the position of the peak maximum slightly shifts from $q = 0.14$ A^{-1} to $q = 0.15$ A^{-1} corresponding to a reduction of the interlayer spacing from 4.5 to 4.2 nm, respectively. It has been shown in the SAXS analysis of HNBR–clay nanocomposites (Fig. 2b) that the interlayer spacing of the clay in HNBR nanocomposites is 4.2 nm. Thus, the reduction of the interlayer spacing of organoclay in the HNBR/(NR–clay masterbatch) blends nanocomposites in dependence on the mixing time is related to the fact that the NR chains available in the clay galleries were gradually replaced by the HNBR chains. The clay is considered as migrated into the HNBR phase. This organoclay migration is nicely co-related with the increase of OMEC in Fig. 5a, which could only be possible if clay migrates from NR (non-polar) phase to HNBR (polar).

The development of the blend morphology in HNBR/(NR–clay master batch) has been qualitatively characterized by using AFM as shown in Fig. 6. AFM images of sample taken out at 2, 3, 15, and 40 min are presented in Fig. 6a–d. The analysis of the AFM photographs shows that there is clay immigration from NR-phase to HNBR-phase takes place. At 2 min of mixing time, a number of clay agglomerates (black points) with a size of nearly 500 nm is visible in the NR-phase (light area) and no clay in the HNBR-phase (dark area) as shown in Fig. 6a. With increasing mixing time, more and more clay moves into the HNBR-phase. It reveals clearly that in start of mixing process, there is dominant localization of the clay tactoids in the NR-domains. Before 15 min predominantly there is the co-continuous morphology. After 15 min mixing time the HNBR component begins to form the island phase. However, after 40 min of mixing time island–matrix morphology, with NR as matrix and HNBR as island with most of organoclay, is obtained.

The experimental results of morphological analysis have a quite coincidence with OMEC. The AFM analysis shows that melt mixing of NR–clay masterbatch with HNBR led to immigration of clay from NR to HNBR-phase which facilitate the ionic conduction in the blend. The migration of organoclay to HNBR-phase could be due to higher affinity of organoclay with polar phase, i.e., HNBR as compared to non-polar phase, i.e., NR. The preferential localization of clay in a specific phase with higher polarity was also observed by Hong et al. [11] or Mehrabzadeh et al. [14]. As the mixing time is increased, clay transfers to HNBR-phase where it is thermodynamically stable with minimum chemical potential. For 40 min of mixing time most of clay has migrated to HNBR-phase. Morphology of a multiphase system is generally determined by viscosity of the components. The organoclay significantly influences the development of blend morphology. The migration of clay increases the viscosity of the HNBR-phase and also influences the interfacial tension of this polar phase. The

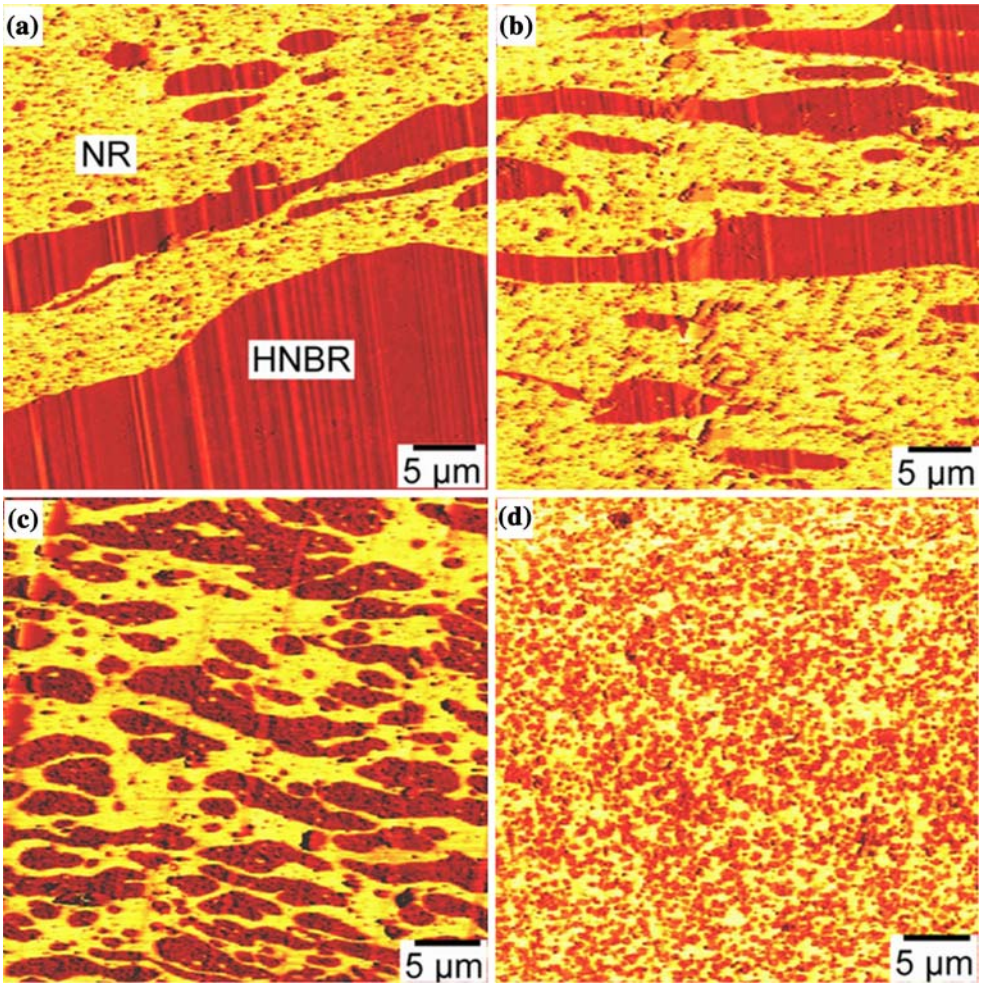

Fig. 6 Development of blend morphology and clay transfer in HNBR/(NR–clay masterbatch) blend in dependence on mixing time: **a** 2 min, **b** 3 min, **c** 15 min, **d** 40 min

AFM analysis shows that the morphology of blend changes from very rough and co-continuous to well refined island–matrix morphology.

The previous hypothesis based on OMEC, SAXS analysis and AFM about a preferential location of the clay within the more polar HNBR of the binary blend needs to be critically analyzed by means of further morphological analyses. Therefore, TEM was employed to inspect the nanostructure of the HNBR/(NR–clay masterbatch) blends. TEM images of randomly microtomed sample of HNBR/(NR–clay masterbatch) blend after 40 min mixing time is shown in Fig. 7. A complex morphology both on micro- and nano-scale can be noticed. The global morphology of the blend after 40 min mixing time has been analyzed at low magnification as shown in Fig. 7a. The clay appears as deep dark features in the dark grey dispersed phase, on the micron size. The higher magnification of the TEM image is shown in the Fig. 7b. This micrograph confirmed the assumption of preferential localization of organoclay stacks with thickness of few tens of nanometers in HNBR-phase.

Figure 7a shows the global view of the blend morphology whereas Fig. 7b shows the nanostructure of blend morphology and localization of clay platelets in the TEM images are in good agreement with the AFM and SAXS investigations. Also becomes clear that the clay migration causes a refinement of the blend morphology. The position of SAXS peaks shift to higher intensity and higher scattering vector.

The inhomogeneous distribution of organoclay in the binary blends gives rise to the interfacial tension gradient and results in a tension gradient [46, 47]. Moreover, the steric repulsion of organoclay at the interface suppresses the coalescence caused by thermal Brownian motion and collision caused by hydrodynamic force. The relevant non-homogeneity detected on microscale indicates that the filler is predominantly confined into well-defined micron-sized volumes. Recently, Hong et al. [11] have studied the

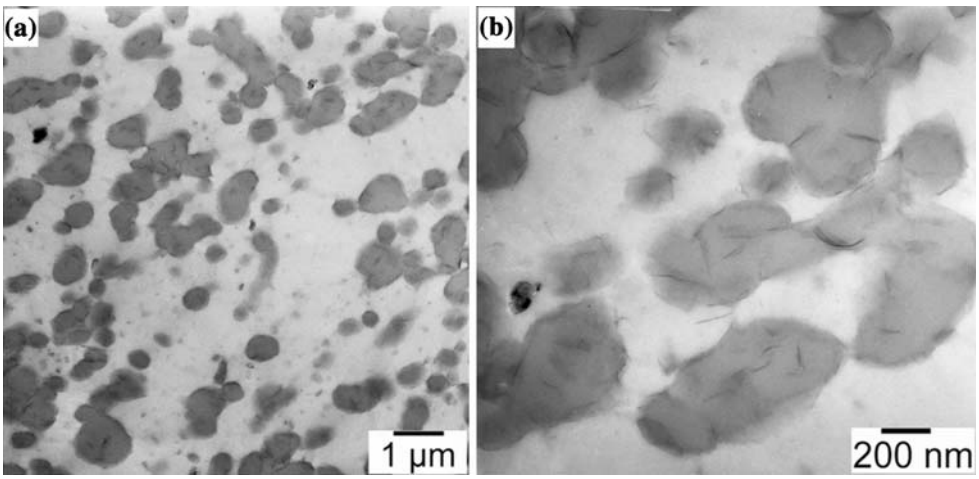

Fig. 7 TEM images HNBR/(NR–clay masterbatch) blends after 40 min of mixing time **a** at lower magnification, **b** higher magnification (*Dark grey* areas of the dispersed phase represent the HNBR-phase, *light grey* area of the matrix represents the NR phase and the black inclusions in the dispersed phase represent to clay platelets)

morphology of blends of PBT/PE–clay nanocomposites. They have shown on the basis of morphological investigation that all the clay is located in the more polar phase, i.e., PBT or at the interface, but not in the non-polar PE phase. The preference of the clay existing in a preferred phase is due to the difference of polarity between organoclay with the polymer chains [48, 49].

Indeed, after 15 min the continuous HNBR-phase starts to divide into domains that partly interrupt the motion of ionic species throughout the matrix. As a result the OMEC subsequently decays in the period between 15 and 40 min. The extent of the conductance decay correlates with the reduction of the domain size of HNBR. In this period the diameter of HNBR-domain reduces from about 2–0.7 μm and the corresponding OMEC from 8.26–6.86 $\times$ 10^{-5} mS.

The reduction of the HNBR-domain size is well known as a result of the compatibilization efficiency of organoclay [14, 18, 19]. The addition of organoclay into HNBR and NR alters their surface tension strongly because of the existence of the surfactant ions which are released from the clay galleries during compounding. That is related to the extent of the released surfactant with the mixing time. In HNBR/(NR–clay masterbatch) blend the interfacial tension reduces drastically when clay migrates from the NR phase to the HNBR-phase. Thus, it can be summarized that the morphology is mainly driven by the compatibilization effect of organoclay.

Conclusion

Investigations on organoclay filled XHNBR and HNBR compounds have shown that it is possible to use the method of OMEC for a successful characterization of the kinetics of the dispersion processes during compounding of such polymer–nanofiller systems. The conductance observed is of ionic nature. The OMEC increases swiftly after addition of organoclay in the polymer matrix and reaches a constant value after a certain time. The plateau of the OMEC corresponds to the constant morphology of rubber–clay nanocomposites. The samples were taken out along the mixing time and analyzed by means of AFM, TEM, and SAXS in terms of the dispersion and distribution of the organoclay. The strong correlation between the OMEC and the filler dispersion delivered an effective tool for the investigation of the organoclay dispersion (intercalation/exfoliation) in polymer melts. The method of OMEC has also been successfully applied for the characterization of the morphology development and the kinetics of clay distribution in rubber blends during the mixing process. The structural background of the conductance curve was discussed by taking into consideration the results of different structural investigations like AFM, SAXS, and TEM measurement. Based on the chart of the OMEC received by mixing pure HNBR with NR–clay masterbatch the clay migration from the NR-phase to the HNBR-phase as a result of favorable interaction of clay to the HNBR-phase and the change of blend morphology as a result of the compatibilization effect of clay was described.

Acknowledgements The authors wish to thank the German Research Foundation (DFG) and the Higher Education Commission Pakistan (HEC) for the financial support of this work. The group of Prof. Georg H. Michler (Institute of Physics, Martin Luther University, Halle-Wittenberg, Germany) for TEM and Prof Thomas Thurn-Albrecht (Institute of Physics, Polymer Physics, Martin Luther University, Halle-Wittenberg, Germany) for discussion of SAXS investigation are highly acknowledged.

References

1. Ogawa M, Takizawa Y (1999) Chem Mater 11:30
2. Wu J, Lerner M (1993) Chem Mater 5:835
3. Fornes TD, Yoon PJ, Keskkula H, Paul DR (2001) Polymer 42:9929

4. Reichert P, Nitz H, Klinke S, Brandsch R, Thomann R, Mülhaupt R (2000) Macromol Mater Eng 275:8
5. Gu SY, Ren J, Wang QF (2004) J Appl Polym Sci 91:2427
6. Gopakumar TG, Lee JA, Kontopoulou M, Parent JS (2002) Polymer 43:5483
7. Lagaron JM, Catala R, Gavara R (2004) Mater Sci Technol 20:1
8. Chang JH, An YUJ (2002) J Polym Sci Polym Phys 40:670
9. Ma J, Qi ZY (2001) J Appl Polym Sci 82:3611
10. Khatua BB, Lee DJ, Kim HY, Kim JK (2004) Macromolecules 37:2454
11. Hong JS, Kim YK, Ahn KH, Lee SJ, Kim C (2007) Rheol Acta 46:469
12. Chow WS, Ishak ZA, Ishiaku US, Karger-Kocsis J, Apostolov AA (2004) J Appl Polym Sci 91:175
13. Li Y, Shimizu H (2004) Polymer 45:7381
14. Mehrabzadeh M, Kamal MR (2002) Can J Chem Eng 80:1083
15. Fang Z, Harrats C, Moussaif N, Groeninck G (2007) J Appl Polym Sci 106:3125
16. Ray SS, Pouliot S, Bousmina M, Utracki LA (2004) Polymer 45:8403
17. Si M, Araki T, Ade H, Kilcoyne ALD, Fisher R, Sokolov JC, Rafailovich MH (2006) Macromolecules 39:4793
18. Gelfer MY, Song HH, Liu L, Hsiao BS, Chu B, Rafailovich M, Si M, Zaitsev V (2003) J Polym Sci Polym Phys 41:44
19. Wang Y, Zhang Q, Fu Q (2003) Macromol Rapid Commun 24:231
20. Kurian YP, Zhang LQ, Wang YQ, Liang Y, Yu DS (2001) J Appl Polym Sci 82:2835
21. Sadhu S, Bhowmick AK (2005) J Mater Sci 40:1633. doi: 10.1007/s10853-005-0663-2
22. Kim J, Oh T, Lee D (2003) Polym Int 52:1058
23. Cho JW, Paul DR (2001) Polymer 42:1083
24. Dennis HR, Hunter DI, Chang D, Kim S, White J, Cho JW, Paul DR (2001) Polymer 42:9513
25. Nah CW, Ryu HJ, Han SH, Rhee JM, Lee MH (2001) Polym Int 50:1265
26. Wang K, Liang S, Du RN, Zhang Q, Fu Q (2004) Polymer 45:7953
27. Van der Hart DL, Asano A, Gilman JW (2001) Chem Mater 13:3781
28. Loo LS, Gleason KK (2003) Macromolecules 36:2587
29. Le HH, Qamer Z, Ilisch S, Radusch H-J (2006) Rubber Chem Technol 79:621
30. Le HH, Kasaliwal GR, Ilisch S, Radusch H-J (2009) Kautsch Gummi Kunstst (in press)
31. Kortaberria G, Solar L, Jimeno A, Arruti P, Gomez C, Mondragon I (2006) J Appl Polym Sci 102:5927
32. Hussain F, Chen JH, Hojjati M (2007) Mater Sci Eng A 445:467
33. Aranda P, Galvan JC, Casal B, Ruehitzky E (1992) Electrochim Acta 37:1573
34. Le HH, Ali Z, Ilisch S, Radusch H-J (2007) In: Proceedings of Technomer 2007, Chemnitz, Germany, 15–17 Nov 2007, p 29 and CD
35. Ali Z, Le HH, Ilisch S, Radusch H-J (2009) J Appl Polym Sci 113:667
36. Bur AJ, Lee YH, Roth SC, Start PR (2005) Polymer 46:10908
37. Sadhu S, Bhowmick AK (2004) J Polym Sci Polym Phys 42:1573
38. Park J, Jana S (2003) Macromolecules 36:8391
39. Shiga S, Furuta M (1985) Rubber Chem Technol 58:1
40. Gatos KG, Sawanis NS, Apostolov AA, Thomann R, Karger-Kocsis J (2004) Macromol Mater Eng 289:1079
41. Wu YP, Jia QX, Yu DS, Zhang LQ (2003) J Appl Polym Sci 89:3855
42. Schön F, Thmann R, Gronski W (2002) Macomol Symp 189:105
43. Kim J, Oh T, Lee D (2004) Polym Int 53:406
44. Wu YP, Zhang LQ, Wang YQ, Liang Y, Yu DS (2001) J Appl Polym Sci 82:2842
45. Kojima Y, Fukumori K, Usuki A, Kurauchi T (1993) J Mater Sci Lett 12:889
46. Lyu S, Jones TD, Bates FS, Macosko CW (2002) Macromolecules 35:7845
47. Sundararaj U, Macosko CW (1995) Macromolecules 28:2647
48. Alexander M, Dubois P (2000) Mater Sci Eng 28:1
49. Giannelis EP, Krishnamoorti R, Manias E (1999) Adv Polym Sci 138:107